ELSEVIER

Contents lists available at ScienceDirect

# Proceedings of the Combustion Institute

journal homepage: www.elsevier.com/locate/proci





# Shock-tube study of the oxidation of ammonia by N<sub>2</sub>O

Olivier Mathieu\*, Claire M. Grégoire, Eric L. Petersen

J. Mike Walker '66 Department of Mechanical Engineering, Texas A&M University, College Station, TX, USA

ARTICLE INFO

Keywords: Ammonia N<sub>2</sub>O Shock tube Laser absorption

#### ABSTRACT

The oxidation of ammonia by N2O was studied by following the time history of ammonia in a shock tube with a spectroscopic laser diagnostic. Dilute (99.5 % Ar) mixtures were studied around atmospheric pressure for several equivalence ratios: 0.25, 0.85, 1.0, and 2.0. The time at which the ammonia concentration reaches 50 % of its original value ( $\tau_{50\%}$ ) was also measured. Results were compared to several detailed kinetics models from the literature. Based on past work from the authors and a literature mechanism, a tentative model was also assembled to better represent the experiments at the conditions investigated herein. The quantitative NH3 diagnostic shed light on the limitations associated with the passivation method to counterbalance ammonia adsorption on the reactor's surface and showed that an ammonia diagnostic is necessary and critical to know the initial conditions for dilute mixtures. Experimental results show a relatively large effect of the equivalence ratio on the mixture's reactivity. The main outcome of this study is that while  $\tau_{50\%}$  can be accurately predicted by all models considered, large variations are observed when comparing with the full NH3 time-history profile. Key features of the experimental profiles were not captured by the models, and large variations were observed between the models. Overall, the most recent models and the tentative models from this study performed the best, but more work remains necessary to fully capture the oxidation of ammonia by N2O. The effect of the third-body collision coefficient on  $N_2O(+M) \subseteq N_2 + O(+M)$  was investigated for several species, but no effect was found under the conditions investigated. However, it is likely that studying  $N_2O$  (+NH<sub>3</sub>)  $\leftrightarrows N_2 + O$  (+NH<sub>3</sub>) is necessary for real-world applications.

## 1. Introduction

Ammonia (NH<sub>3</sub>) is one of the most produced chemicals due to its importance as a fertilizer as well as its use in many other industries such as refrigeration, pharmaceutical, textile, and explosives [1]. Over the past few years, due to concerns over climate change, much research on NH<sub>3</sub> combustion has been performed [2,3] because of the attractiveness of its carbon-free nature and its advantageous storage properties compared to hydrogen. This research showed that (i) ammonia has overall poor combustion properties [2], probably necessitating co-firing with another fuel; and (ii) that most chemical kinetics models still require further development [3-5]. The need for further development of the model is particularly evident when comparing literature models with species time-history profiles [6-8].

The use of ammonia as a fuel can also lead to high levels of NOx (NO, NO<sub>2</sub>, but also N<sub>2</sub>O) emissions during its combustion [2]. NO and NO<sub>2</sub> are regulated, toxic pollutants that can contribute to the formation of ozone in the lower atmosphere and to acid rain. N<sub>2</sub>O, on the other hand, is not

directly harmful to humans but has a global warming potential 300 times larger than  $CO_2$  over a 100-year period and contributes significantly to the depletion of the tropospheric ozone layer [9].  $N_2O$  is in fact a combustion intermediate of ammonia [2,7] and, with such a large global warming potential,  $N_2O$  emissions should be strongly limited for practical applications using ammonia as a fuel if global warming mitigation is intended.

In stationary applications like gas turbines or boilers, a two-stage combustion process is often considered to avoid NOx emissions [10]. In the primary zone of a two-stage combustion process, ammonia is burned in a fuel-rich environment, producing low NOx emissions. However, while NOx emissions are limited in fuel-rich flames, any device operating under such conditions would suffer from an inefficient combustion process, with unburned fuel emissions (ammonia,  $H_2$ , and other combustion intermediates). The role of the secondary zone is to burn this unreacted fuel by injecting air, to both limit emissions and improve burning efficiency. In an internal combustion engine, a fraction of the burned gas remains in the cylinder at the end of the exhaust

E-mail address: olivier.mathieu@tamu.edu (O. Mathieu).

<sup>\*</sup> Corresponding author.

stroke. This residual exhaust gas contains unburnt fuel, combustion intermediates and products, and is then mixed with the fresh charge during the intake stroke.

In both applications, interactions between ammonia and N2O can thus be anticipated, and it is therefore important to understand these interactions at the fundamental combustion chemistry level. To the best of the author's knowledge, only a limited number of studies focused on NH<sub>3</sub>/N<sub>2</sub>O interactions during combustion. In terms of global kinetics data, the ignition delay time of the NH<sub>3</sub>/N<sub>2</sub>O system was measured in a shock tube by Fujii et al. [11] and in a rapid compression machine by Liao et al. [12], whereas laminar flame speeds were measured by Han et al. [13]. While global kinetics data are useful to assess the overall reactivity of a system, they are not as valuable as speciation profiles, such as those measured for NH3, N2O, and NO during NH3/N2O oxidation by Cornell et al. [14]. In this study, large differences between the predictions of various models were observed, especially for NO for the 850-1180 K range. Lastly, concentration time histories of key species add another level of constraint to validate detailed kinetics models, as evidenced by the work of Alturaifi et al. [6-8]. Such a type of data is therefore desired, and it is worth mentioning the precursor study of Salimian et al. [15], where concentration histories of NH<sub>3</sub>, N<sub>2</sub>O, H<sub>2</sub>O, NO, and OH were measured during NH<sub>3</sub>/N<sub>2</sub>O oxidation in a shock tube. Unfortunately, only a limited number of profiles are available in this paper, and the data were collected after the incident shock wave, in less ideal conditions than those behind the reflected shock wave where the gas is not subject to any motion. Lastly, note that the detonation in NH<sub>3</sub>/N<sub>2</sub>O mixtures was recently investigated experimentally by Weng et al. [16].

The aim of the present study was thus to provide such time-history profiles behind reflected shock waves, to further study the interactions between NH $_3$  and N $_2$ O during combustion. To simplify the system and to exacerbate these interactions, this study focused on the direct oxidation of ammonia from N $_2$ O over a wide range of equivalence ratios by following the time history of ammonia with a spectroscopic diagnostic. In such a system, as mentioned by Salimian et al. [15], the rate-limiting initial step of this system corresponds to the formation of O radicals from the unimolecular decomposition of N $_2$ O. As further discussed in this paper, this initial interaction between NH $_3$  and O allows the study of ammonia oxidation with a different initiation pathway than for NH $_3$ /O $_2$  mixtures, and at typically lower temperatures.

First is presented the shock-tube apparatus and spectroscopic diagnostic used, followed by a presentation of the experimental results and a comparison with models from the literature. A tentative model was assembled, and the results are discussed using this model.

## 2. Experimental setup

## 2.1. Shock-tube facility

Experiments were conducted in a stainless-steel shock tube. Details of the apparatus are available in the literature [6], and only a brief description is provided herein. The shock tube has a 6.78-m long driven section and a 3.0-m long driver section (16.2 cm and 7.62 cm i.d., respectively). The two sections were separated with polycarbonate diaphragms (0.254-mm thickness). The driven section was vacuumed to a pressure of  $\sim 10^{-3}$  Pa or better prior to each experiment using a combination of a mechanical pump and a turbomolecular pump. Five piezoelectric pressure transducers, mounted along the last 2 m of the driven section, were used to monitor the propagation of the incident shock wave and extrapolate its velocity to the endwall location. This velocity, in conjunction with the initial driven-section gas temperature and pressure, was used to calculate the temperature ( $T_5$ ) and pressure ( $P_5$ ) behind the reflected shock wave. The estimated uncertainty in  $T_5$  and  $P_5$  are 0.8 % and 1.0 %, respectively [17].

Mixtures were prepared in a separate stainless-steel tank via the partial pressure method. All gasses were supplied by Praxair with a

purity level of 99.995 % for  $N_{\rm H_3}$ , 99.5 % for  $N_{\rm 2O}$ , and 99.999 % for Ar. Four different equivalence ratios ( $\phi$ ) were investigated in this study: 0.25, 0.85, 1.0, and 2.0 in 99.5 % Ar dilution (using  $N_{\rm 2}$  and  $H_{\rm 2O}$  as final products for the equivalence ratio calculation). Note that these equivalence ratios are average equivalence ratios only due to the run-to-run variation in the passivation procedure, and the exact composition for each experiment is provided in Supp. Mat.

The aforementioned passivation procedure was needed in this study since ammonia adsorbs on stainless steel and a very high dilution level is used. The passivation procedure consists of introducing pure ammonia first to passivate the wall of the shock tube and then vacuuming out this ammonia prior to adding the mixture to study (for the mixture preparation in the mixing tank, ammonia was introduced first and allowed to rest for a few minutes, so  $\mathrm{NH}_3$  can adsorb and not affect the preparation). Ideally, after this passivation stage, the stainless steel is saturated with ammonia and the remaining gaseous ammonia introduced is all vacuumed before introducing the mixture. In reality, as described in Alturaifi et al. [6], the passivation method is not sufficient in itself to guarantee the intended concentration of ammonia when dealing with very dilute mixtures, and a small but noticeable variation in the initial ammonia concentration could still be observed. This variation in the NH<sub>3</sub> concentration could be due to several factors such as the exact resting and pumping times during the passivation procedure, the variation in the temperature of the shock tube, the time between the filling of the driven section and the experiment, etc. In fine, for very dilute mixtures, the authors believe that it is necessary to measure the NH3 mole fraction prior to each experiment to ensure accurately known initial conditions. Lastly, it is worth mentioning the study of Feng et al. [18], where it was demonstrated that NH<sub>3</sub> decomposes on stainless steel for metal surface temperatures as low as 700 K. In our study, and in shock tubes in general, while the gas temperature reaches high temperatures, the inner surface temperature of the tube wall - where NH3 is adsorbed - barely increases due to the short duration of the experiment, relatively slow heat transfer mechanisms, and the high thermal inertia of the tube material. As a result, no interaction between the NH<sub>3</sub> adsorbed on the shock-tube wall and windows with the laser diagnostics was anticipated, nor observed.

## 2.2. NH<sub>3</sub> laser absorption diagnostic

To measure the NH $_3$  mole fraction prior to and during our experiments, a tunable quantum cascade laser (QCL) that generates narrow-linewidth light near 10.4  $\mu$ m was used. The QCL was tuned to 957.839 cm $^{-1}$  to access the sQ(12,12) transition in the  $\nu_2$  fundamental band of NH $_3$ . The generated light was split into incident ( $I_0$ ) and transmitted ( $I_t$ ) beams using a ZnSe flat beamsplitter. The intensities of the beams were monitored via two, 1-MHz bandwidth HgCdTe photovoltaic detectors (InfraRed Associates). Bandpass filters centered on 10,400 nm (FWHM 100 nm) and 10,177 nm (FWHM 708 nm), were used to cover the detectors receiving  $I_t$  and  $I_0$ , respectively. The frequency of the light was frequently monitored using a flip mirror to send the laser beam to a wavemeter (Bristol 671).

The transmission signal ratio  $(I_t/I_0)$  was used to both determine the initial NH<sub>3</sub> mole fraction present in the mixture after filling the driven section and to follow the NH<sub>3</sub> speciation profile at the high-temperature test conditions. In each case, the Beer-Lambert law was used to calculate the time-varying NH<sub>3</sub> mole fraction  $(X_{NH_3}(t))$  with the time-varying absorption coefficient  $(k_v(t))$ , the time-varying total mixture pressure (P(t)), and the path length (L) as known factors:

$$I_t/I_0 = \exp\left[-k_{\nu}(t)\cdot X_{NH_3}(t)\cdot P(t)\cdot L\right] \tag{1}$$

The absorption coefficient at room temperature can be calculated using the known line strength and line shape of the sQ(12,12) transition at 296 K provided in Alturaifi and Petersen [19]. More details about this diagnostic are available in [6], and its uncertainty is within  $\pm 12\%$  [6].

#### 3. Results and comparison with models

In this section, the NH3 time histories are presented for each equivalence ratio investigated. Some selected time-history profiles are then compared to detailed kinetics models from the literature to assess their performance. In addition, the time at which 50 % of NH<sub>3</sub> ( $\tau_{50\%}$ ) is consumed was measured from the NH3 profiles, to assess the overall reactivity of the models. Selected models from the literature were X. Zhang et al. [20] (KAUST); Mathieu and Petersen [21]; Nakamura et al. [22]; Y. Zhang et al. [23]; Otomo et al. [24]; Wang et al. [25]; Gotama et al. [26]; Thomas et al. [27]; Jian et al. [28]; and Stagni et al. [29]. For the purpose of the numerical analysis in the discussion section, a tentative model was also assembled in this study. This model consists of the H<sub>2</sub>/O<sub>2</sub> chemistry from NUIGMech 1.1 [30], the NH<sub>3</sub> pyrolysis sub-mechanism from Alturaifi et al. [6], which was validated in similar conditions to the results obtain during this study; the NH<sub>3</sub>/NOx mechanism from KAUST [20], which predicted relatively accurately the N<sub>2</sub>O profiles during NH<sub>3</sub> oxidation when coupled with the Alturaifi et al. pyrolysis sub-mechanism, along with modifications suggested in [7]; and the low-pressure limit reaction rate coefficient for  $N_2O(+M) \leq N_2 +$ O (+M) (R1) measured under the same conditions and in the same apparatus as this study by Mulvihill et al. [31]. Note that the tentative model was successfully tested against other NH3 data from our group [6-8] but not against other data sets available from the literature. Note also that all the comparisons between the experimental profiles and models that are not presented in the present paper are available in the Supplementary Material section. Chemkin Pro 17.2 was used to model these data using the 0-D, closed, homogeneous, batch reactor module with the "Constrain volume and solve energy equation" solver assumption.

#### 3.1. $\phi = 0.25$ condition

The time-history profiles obtained during this study for NH $_3$  at  $\varphi=0.25$  are visible in Fig. 1. As can be seen, due to the aforementioned difficulties in passivating the inner surface of the apparatus with ammonia in a truly consistent way, the initial NH $_3$  concentration varies between about 600 and 850 ppm (leading to an equivalence ratio varying between 0.20 and 0.30 ( $\varphi=0.24$  in average)). Concerning the profiles, the NH $_3$  oxidation occurs at a rate that increases with the temperature, and NH $_3$  appears to be fully oxidized within the time frame of our experiments at temperatures above 1600–1615 K.

The comparison with the models and the  $NH_3$  profile at 1569 K is visible in Fig. 2. As can be seen, all models predict the overall trend of the data. However, a few models are under-reactive, notably the Nakamura one, while the Thomas et al., Mathieu and Petersen, and X. Zhang et al. models present almost similar predictions. The Stagni et al. model accurately predicts the results, closely followed by the tentative

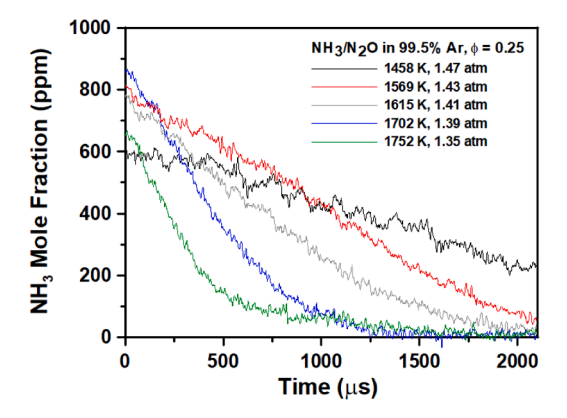


Fig. 1. Evolution with temperature of NH $_3$  time-history profiles for NH $_3$ /N $_2$ O mixtures in 99.5 % Ar at  $\varphi=0.25$ .

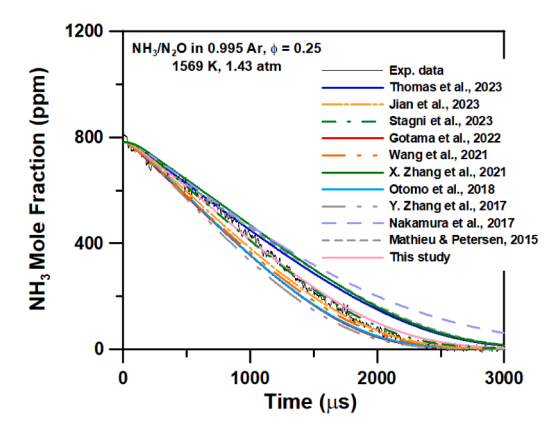


Fig. 2. NH<sub>3</sub> time-history profile at 1569 K and 1.43 atm and comparison with detailed kinetics models for a NH<sub>3</sub>/N<sub>2</sub>O mixture in 99.5 % Ar at  $\phi=0.25$ .

model of the present study and the Jian et al. model, in terms of accuracy. Note the improvement made by the few modifications of the KAUST (X. Zhang et al.) model, when compared with the tentative model.

## 3.2. $\phi = 0.85$ condition

For the  $\varphi=0.85$  condition, Fig. 3, similar trends are observed overall. However, one can see that the ammonia profile reaches the zero level in a very slow fashion after the first rapid decrease. For example, the NH $_3$  concentration fell from about 1650 ppm to about 200 ppm in 250  $\mu s$  at 2153 K, but then the NH $_3$  concentration decreased from 200 ppm to about zero in more than 2 ms.

This peculiar feature of the experimental profile is interestingly not captured by any of the models tested. As can be seen, the first rapid decrease in the NH<sub>3</sub> concentration is captured by the models (best predicted by the tentative model), but they predict a full consumption of ammonia, and not this slow decrease when NH<sub>3</sub> reaches about 200 ppm.

## 3.3. $\phi = 1.0$ condition

Concerning the stoichiometric case, the behavior observed is close to what has been seen for the  $\varphi=0.85$  condition in that, at sufficiently high temperatures (between 1680 and 1862 K, as per Fig. 5), a slowly declining plateau is reached after a period of very rapid decrease in the ammonia level. However, the rate at which NH $_3$  is consumed in these slowly declining plateaus (observed for 65–150 ppm of NH $_3$ ) is then rapidly increasing past around 1.5 ms until the ammonia is fully consumed.

The comparison between a stoichiometric profile (1680 K, 1.40 atm)

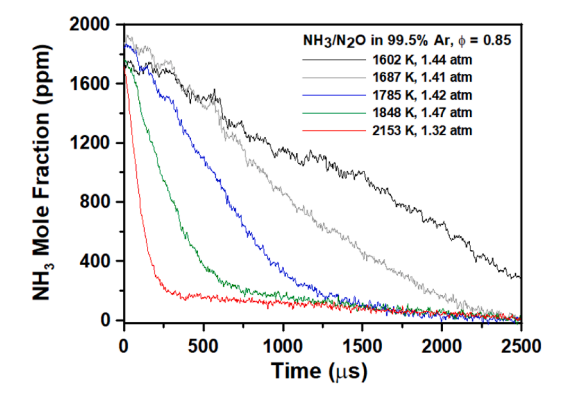


Fig. 3. Evolution with the temperature of NH $_3$  time-history profiles for NH $_3/$  N $_2O$  mixtures in 99.5 % Ar at  $\varphi=0.85.$ 

and the detailed kinetics models is visible in Fig. 6. As can be seen, models are somewhat missing the overall shape of the experimental profile, as they predict an  $NH_3$  consumption that is too rapid at the beginning (first 700  $\mu s$ ) and then underpredict the rate at which  $NH_3$  is consumed, leading to an overprediction of the  $NH_3$  concentration when the ammonia is fully consumed experimentally at around 2.5 ms.

## 3.4. $\phi = 2.0$ condition

The experimental NH $_3$  profiles for the fuel-rich case are visible in Fig. 7. A similar behavior to the other equivalence ratios is observed except that the ammonia is not fully consumed within the timeframe of the experiment (at least through pyrolytic reactions since the mixture is oxygen deficient) and reached a slowly decreasing plateau at around  $250 \pm 50$  ppm. Note that the initial NH $_3$  concentration almost did not vary from one experiment to the other, due to the larger amount of NH $_3$  in the  $\varphi=2.0$  mixture, making it less sensitive to variation in the passivation method effectiveness.

Comparing an experimental profile with the models for the  $\varphi=2.0$  condition, Fig. 8, shows that while the overall trend is captured, there is a large discrepancy amongst the models concerning the predicted value of NH $_3$  at the plateau after the rapid consumption phase, between about 0 ppm for the Y. Zhang et al. model, and 530 ppm for the Mathieu and Petersen and Thomas et al. models. A factor of about three is still observed between the most recent models of Thomas et al. and Jian et al. A few models are predicting the final NH $_3$  level quite accurately, but the tentative model of the present study is the closest overall, when considering the full profile. Notably, no model captures the rapid transition between the rapid decrease in the NH $_3$  concentration and the slow decaying plateau observed experimentally.

## 3.5. $\tau_{50\%}$ results

To assess the overall reactivity of the models selected, the time at which 50 % of the ammonia is consumed  $(\tau_{50\%})$  is visible in Fig. 9 for the stoichiometric condition (other conditions show similar results and are available in SM). As can be seen, extracting these data from the profiles shows that all selected models are accurately predicting the reactivity of the mixture with the temperature (corresponding to the slope), and are all within a factor of less than two with the data (with the most recent models being slightly more accurate overall). These results illustrate the fact that, while these types of data (equivalent to a classical ignition delay time measurement) are necessary, it can also be misleading since one could conclude from Fig. 9 that all models can be used to predict the combustion of the NH<sub>3</sub>/N<sub>2</sub>O system, which is a conclusion that cannot be fully reached when comparing with the full profiles, as seen in Figs. 2, 4, 6, and 8.

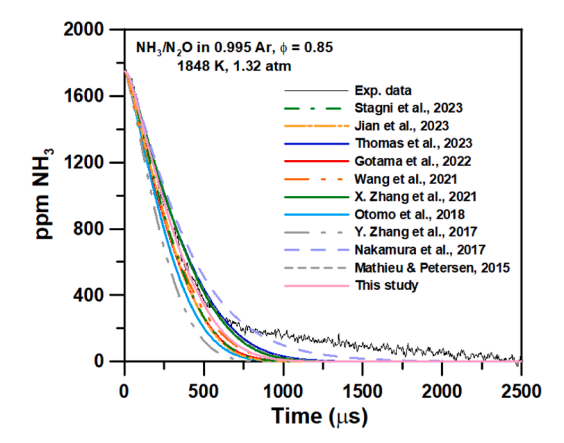


Fig. 4. NH<sub>3</sub> time-history profile at 1848 K and 1.32 atm and comparison with detailed kinetics models for a NH<sub>3</sub>/N<sub>2</sub>O mixture in 99.5 % Ar at  $\phi=0.85$ .

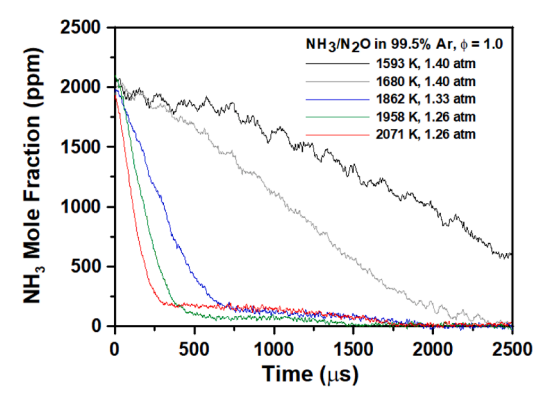


Fig. 5. Evolution with temperature of NH $_3$  time-history profiles for NH $_3$ /N $_2$ O mixtures in 99.5 % Ar at  $\varphi=1.0$ .

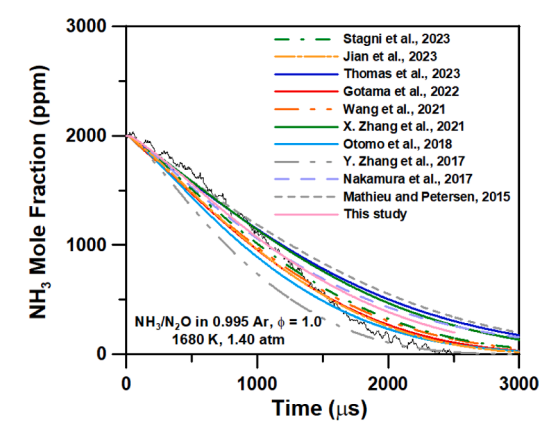


Fig. 6. NH<sub>3</sub> time-history profile at 1680 K and 1.40 atm and comparison with detailed kinetics models for a NH<sub>3</sub>/N<sub>2</sub>O mixture in 99.5 % Ar at  $\phi = 1.0$ .

## 4. Discussion

## 4.1. Results analysis

During this study, NH $_3$  was oxidized by N $_2$ O and, as pointed out in the historical study of Salimian et al. [15], the reactivity of this system is initiated and limited by the formation of O radicals from the unimolecular decomposition of N $_2$ O via R1 (N $_2$ O (+M)  $\leftrightarrows$  N $_2$  + O (+M)). Consequently, the oxidation of NH $_3$  can occur at much lower temperatures compared to when O $_2$  is used as an oxidizer.

This behavior is visible by comparing the onset of reactivity from the NH<sub>3</sub> profiles from this study and those from the ammonia pyrolysis [6] and oxidation [8] studies from Alturaifi and coworkers, obtained in similar conditions and in the same apparatus. Indeed, beside the coldest temperature investigated at  $\varphi=0.25$  (1458 K), the NH<sub>3</sub> profiles show a consumption of ammonia right from the very beginning of the experiment with the NH<sub>3</sub>/N<sub>2</sub>O system, for temperatures as low as 1650 K for the fuel-rich case (Fig. 7) or lower for the other conditions. On the other hand, a temperature of at least 2200 K is necessary to see such behavior with NH<sub>3</sub> pyrolysis [6] and higher than 2150 K at  $\varphi=0.56$  when O<sub>2</sub> is used [8].

To understand the chemistry behind the oxidation of NH $_3$  by N $_2$ O, a sensitivity analysis on NH $_3$  was conducted with the tentative model of this study, since it consistently provided the best (or among the best) predictions in our study. Three mixtures were used to cover the entire range of equivalence ratios investigated:  $\varphi=0.25,\ 1.0,\$ and 2.0. A temperature of 1950 K and a pressure of 1.35 atm were selected. The normalized results of this sensitivity analysis are visible in Fig. 10. As one can see, the most sensitive reactions to promote NH $_3$  consumption

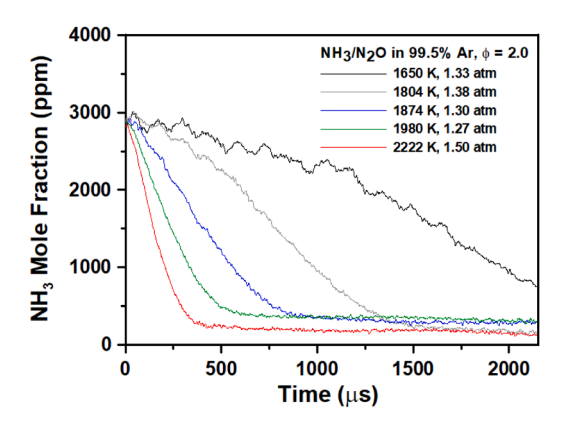


Fig. 7. Evolution with temperature of NH $_3$  time-history profiles for NH $_3$ /N $_2$ O mixtures in 99.5 % Ar at  $\varphi=2.0$ .

are R1, NH $_3$  + OH  $\leftrightarrows$  H $_2$ O + NH $_2$  (R2), NH $_2$  + H $_2$   $\leftrightarrows$  NH $_3$  + H (R3, in reverse), and NH $_3$  + O  $\leftrightarrows$  NH $_2$  + OH (R4). The only reaction reducing the NH $_3$  consumption common to all three conditions is N $_2$ O + H  $\leftrightarrows$  N $_2$  + OH (R5), which is very sensitive for the stoichiometric and fuel-rich conditions.

A reaction pathway analysis was also conducted to understand the peculiar behavior of these NH $_3$ /N $_2$ O mixtures where, after a rapid decrease in the NH $_3$  mole fraction, the mole fraction of NH $_3$  declines very slowly, or even presents a pseudo plateau for the fuel-rich case. Again, this behavior was not observed for NH $_3$ /O $_2$  mixtures [8]. For the stoichiometric and fuel-lean condition, as mentioned above, the reactivity is always initiated by the formation of O radicals through R1 in our system. This radical O will then react with NH $_3$  via R4 and form NH $_2$  and OH. The pool of OH radicals will increase very rapidly and after a few microseconds only, the reaction NH $_3$  + OH  $\leftrightarrows$  NH $_2$  + H $_2$ O (R2) will become important for NH $_3$  consumption, explaining its high sensitivity.

As the pool of NH<sub>2</sub> radicals rapidly builds up via R2 and R4, NH<sub>2</sub> will also react with the O radicals from R1 via  $NH_2 + O \rightleftharpoons HNO + H$  (R6) and, to a lesser extent,  $NH_2 + O \rightleftharpoons NH + OH$  (R7), with the NH from R7 also forming HNO via NH+OH  $\rightleftharpoons$  HNO + H (R8). The HNO from R6 and R8 rapidly decomposes via HNO  $\leq$  NO + H (R9). Thus, there is an important formation of H radicals from R6 and R9, explaining the large sensitivity of the consumption of NH<sub>3</sub> via R3 (NH<sub>2</sub> + H<sub>2</sub>  $\rightleftharpoons$  NH<sub>3</sub> + H, in reverse) in Fig. 10. Importantly, this large formation of H radicals can also promote the formation of NH<sub>3</sub> at later stages via NH<sub>3</sub> +  $M \subseteq$  NH<sub>2</sub> +  $\mathrm{H}+M$  (R10, in reverse). This formation of NH<sub>3</sub> via R10 also reduces the reactivity by acting as a termination reaction, and this mechanism explains the slow decrease in the NH3 profile past the rapid oxidation phase by O atoms. Note that the large formation of H radicals can also induce an important reaction with  $N_2O$  via R5 ( $N_2O + H \Leftrightarrow N_2 + OH$ ), which will prevent the formation of O radicals via R1. Note also the formation of NO via  $N_2O + O \Leftrightarrow NO + NO$  (R11), which will slow down the overall reactivity, with this reaction being among the most sensitive reactions for the lower equivalence ratio investigated, as visible in Fig. 10.

Concerning the first phase of rapid NH $_3$  consumption, note that after 20–30 µs only, NH $_3$  decomposition occurs mainly via NH $_3$  + OH  $\leftrightarrows$  NH $_2$  + H $_2$ O (R2), while R4 (NH $_3$  + O  $\leftrightarrows$  NH $_2$  + OH) remains important. Past 100 µs, the N $_2$ O is almost completely consumed (with now R5 dominating over R1), while NH $_3$  is essentially consumed via R2, and NH $_2$  is mostly consumed by NH $_2$  +H  $\leftrightarrows$  NH + H $_2$  (R12). Note that, for the fuellean case, the large excess of O and OH radicals favors the reverse reaction of R10 (O $_2$  + H  $\leftrightarrows$  O + OH), which then reduces the pool of radicals, leading to an inhibition of NH $_3$  oxidation. It is also important to discuss the fuel-rich case (Figs. 7-8). The reason behind the observed pseudo plateau in NH $_3$  is the temperature range investigated where N $_2$ O allows the oxidation of NH $_3$  at much lower temperatures than O $_2$ . Once N $_2$ O and the associated reactive radicals O/OH are consumed, the

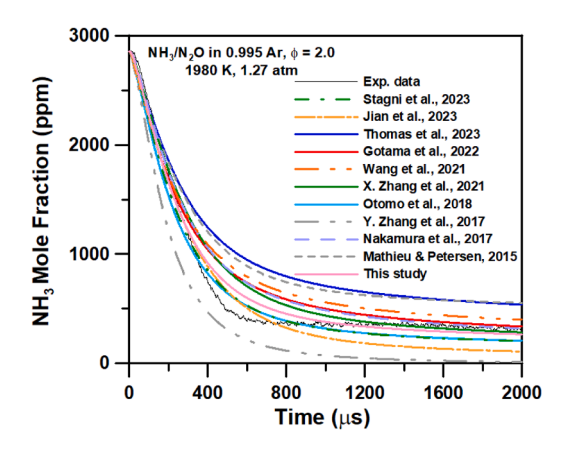


Fig. 8. NH<sub>3</sub> time-history profile at 1980 K and 1.27 atm and comparison with detailed kinetics models for a NH<sub>3</sub>/N<sub>2</sub>O mixture in 99.5 % Ar at  $\phi=2.0$ .

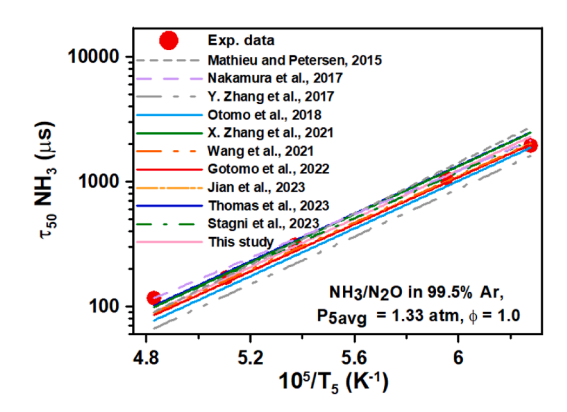


Fig. 9. Evolution with temperature of the time at which 50 % of the NH<sub>3</sub> ( $\tau_{50\%}$ ) is consumed and comparison with models for a NH<sub>3</sub>/N<sub>2</sub>O mixture in 99.5 % Ar at  $\varphi=1.0$ .

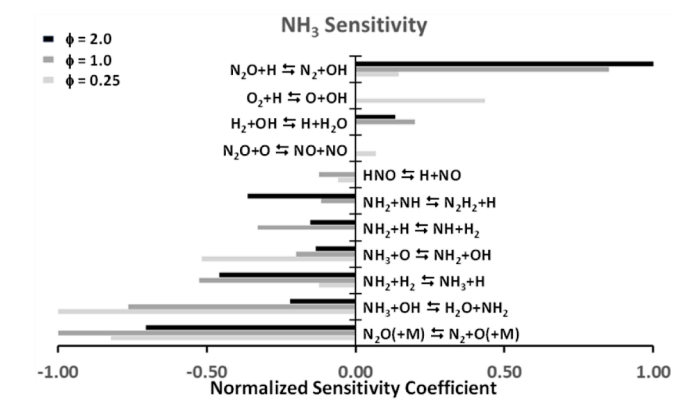


Fig. 10. Normalized sensitivity analysis on NH $_3$  with the tentative model of this study at 1950 K, 1.35 atm, for NH $_3$ /N $_2$ O mixtures in 99.5 % Ar at  $\varphi=0.25$ , 1.0. and 2.0.

remaining  $NH_3$  can only be consumed via pyrolysis reactions, and the highest temperature investigated herein corresponds to the lowest temperatures investigated in our pyrolysis study [6], explaining the very slow decay in the  $NH_3$  mole fraction.

Lastly, the reaction  $NH_2 + N_2O \leftrightarrows N_2H_2 + NO$  significantly influenced  $NH_3$  predictions in some conditions for in the Cornell et al. study for  $NH_3/N_2O$  mixtures in a jet-stirred reactor. They concluded that the rate constant of this reaction was likely overestimated by as much as an order of magnitude. However, dividing the rate coefficient of this

reaction by a factor of 10 did not modify the predictions from the tentative model in our study.

## 4.2. Third body coefficient effect on R1

Here it is important to mention the large effect of the nature of the third body collision partner (the "M" in R1) on the actual reaction rate of R1. Indeed, depending on the chemical species taking the role of the third body, a coefficient is applied to the A factor of R1 by the model. For instance, all the literature models used herein have the following third body coefficients for the following species: 1.7 for  $N_2$ , 1.4 for  $O_2$ , and 12 for  $H_2O$ . To these species and coefficients, the Y. Zhang et al. model [23] adds enhancing coefficients for NO (3.0) and  $N_2O$  (3.5) (note that these additional coefficients were also adopted in Gotama et al. [26]). To investigate the effect of the third body coefficients of NO and  $N_2O$ , the same coefficients used in Y. Zhang et al. were implemented to the tentative model of the present study. Results, visible in Fig. 11, show that adding these third body coefficients has no appreciable effect on the model's predictions in the conditions investigated herein.

Interestingly, the recent work from Harada et al. [32] showed that the third body coefficient of 12 for  $H_2O$  is a large overestimation, leading to too fast of a rate of dissociation for N2O via R1 in their study. They recommended a factor 6.6 instead, and the effect of this recommended third body coefficient is also visible in Fig. 11. As one can see, no effect can be seen as well under the conditions of our study. Lastly, since NH<sub>3</sub> is used as a fuel and can act as a third body with N2O in our study, a third body coefficient was implemented for NH<sub>3</sub>. A value of 6.6, similar to the value determined for H2O in the work from Harada et al. was selected due to the close molar mass of the two molecules. Despite this high third body coefficient (compared to 1.7 for N<sub>2</sub> and 1.4 for O<sub>2</sub>), again, no effect was observed on the NH3 profiles' predictions under the conditions of our study. However, note that the third body effects were observed for a 1:18 ratio for N2O:H2O in the Harada et al. study, versus a 1:1.3 at best for the N<sub>2</sub>O and NH<sub>3</sub> proportion in the present study. Therefore, the lack of third body effect in our study was to be anticipated based on the third-body coefficients from the Harada et al. study.

Lastly, one can mention the study of Jasper [33] where collision efficiencies for NH $_3$  were calculated for a few different reactions (but not R1). The third body coefficients for NH $_3$  provided by this study range from  $\sim 9$  to 23 at 2000 K, depending on the reaction considered. A coefficient from 23 was used on R1 which, as visible in Fig. 11, had nearly no effect on the predictions. Again, this lack of effect is due to the highly dilute nature of our study, and a study dedicated to the third body effect on the thermal dissociation of N $_2$ O via N $_2$ O (+ NH $_3$ )  $\rightleftharpoons$  N $_2$  + O (+ NH $_3$ ) is still necessary for less dilute or fuel/air mixtures, to fully understand the importance of ammonia as a third body partner in this system and for real-world applications.

## 5. Conclusions

In this study, the oxidation of ammonia by  $N_2O$  in a shock tube was followed by measuring the  $NH_3$  consumption using a spectroscopic diagnostic. Wide ranges of temperature and equivalence ratio were covered, for near-atmospheric pressure. Results showed a very rapid onset of reactivity initiated by the decomposition of  $N_2O$ , which allowed for studying ammonia combustion at temperatures much lower than when  $O_2$  is used as oxidizer. This rapid decrease in the  $NH_3$  mole fraction was followed by a long period of slow  $NH_3$  consumption, or even a pseudo plateau for the fuel-rich mixture, which was caused by the formation of  $NH_3$  by  $NH_2$  and H radical recombination for the fuel-lean and stoichiometric cases, whereas the excess of  $NH_3$  in the fuel-rich case was undergoing pyrolysis but at a too low of a temperature for its rapid thermal decomposition.

A large selection of models from the literature was assessed using the data. Results of this comparison showed that while the models were accurately predicting a global kinetic property like the time at which 50

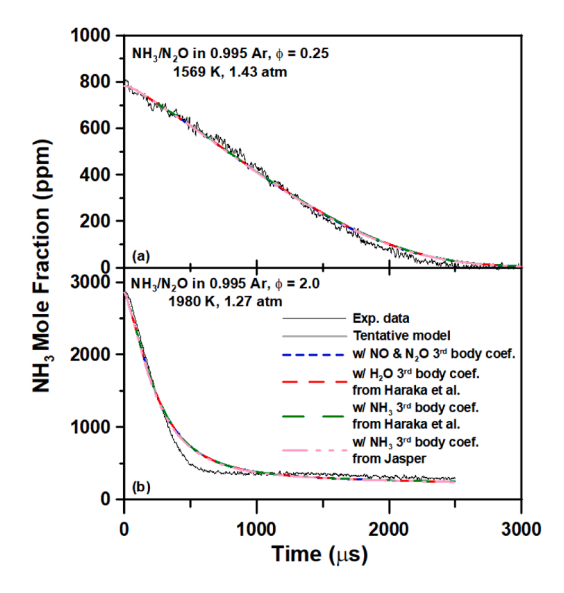


**Fig. 11.** Effect of third body coefficients of  $N_2O$ , NO,  $H_2O$ , and  $NH_3$  on R1 ( $N_2O$  (+M)  $\rightleftharpoons N_2 + O$  (+M) on selected computed  $NH_3$  profiles.

% of the ammonia was consumed, more work is still required to fully predict the NH $_3$  time histories measured herein, as some features are not fully captured by the models.

The numerical analysis showed that the reactivity of the mixture is always initiated by R1:  $N_2O$  (+M)  $\Rightarrow$   $N_2$  + O (+M).

Given the large role of the third body (+M) on this reaction, a systematic study was conducted using a new third body coefficient proposed for  $H_2O$ , or by adding third body coefficients for NO,  $N_2O$ , and  $NH_3$ . No effects were observed, probably due to the range of conditions investigated. However, a fundamental study of the effect of  $NH_3$  as third body still needs to be conducted to possibly improve the predictions in real-world applications where the reactants concentrations will be much larger.

## Novelty and significance statement

The novelty of this research consists of studying the oxidation kinetics of ammonia with  $N_2O$  in a shock tube, by following the time history of ammonia. The  $NH_3/N_2O$  system is of importance for gas turbines (two-stage combustion) and internal combustion engines (residual exhaust gasses) since  $N_2O$  is a combustion intermediate of ammonia and has a very large greenhouse gas potential. It is significant and topical because ammonia is considered as a carbon-free fuel for power and transportation in many countries. The  $NH_3/N_2O$  system has also not been extensively studied.

## **Author contributions**

- OM: wrote the paper, and performed the numerical analysis.
- CMG: measured and post-processed the data.
- ELP: acquired the funding, supervised the project, and reviewed the paper.

#### **Declaration of competing interest**

The authors declare that they have no known competing financial interests or personal relationships that could have appeared to influence the work reported in this paper.

## Acknowledgements

This material is based upon work supported by the National Science

Foundation under Grant No CBET-20308433.

## Supplementary materials

Supplementary material associated with this article can be found, in the online version, at doi:10.1016/j.proci.2024.105250.

#### References

- [1] O. Mathieu, E.L. Petersen, Carbon free fuels, ACS in Focus (2023).
- [2] A.M. Elbaz, S. Wang, T.F. Guiberti, W.L. Roberts, Review on the recent advances on ammonia combustion from the fundamentals to the applications, Fuel Communications 10 (2022) 100053.
- [3] A.G. Szanthoffer, I.G. Zsély, L. Kawka, M. Papp, T. Turányi, Testing of NH<sub>3</sub>/H<sub>2</sub> and NH<sub>3</sub>/syngas combustion mechanisms using a large amount of experimental data, Appl. En. Combust. Sci. 14 (2023) 100127.
- [4] A. Alnasif, S. Zitouni, S. Mashruk, et al., Experimental and numerical comparison of currently available reaction mechanisms for laminar flame speed in 70/30 (% vol.) NH<sub>3</sub>/H<sub>2</sub> flames, Appl. En. Combust. Sci. 14 (2023) 100139.
- [5] A. Alnasif, S. Mashruk, H. Shi, et al., Evolution of ammonia reaction mechanisms and modeling parameters: A review, Appl. En. Combust. Sci. 15 (2023) 100175.
- [6] S.A. Alturaifi, O. Mathieu, E.L. Petersen, An experimental and modeling study of ammonia pyrolysis, Combust. Flame 235 (2022) 111694.
- [7] S.A. Alturaifi, O. Mathieu, E.L. Petersen, Shock-tube laser absorption measurements of N<sub>2</sub>O time histories during ammonia oxidation, Fuel Communications 10 (2022) 100050.
- [8] S.A. Alturaifi, O. Mathieu, E.L. Petersen, A shock-tube study of NH<sub>3</sub> and NH<sub>3</sub>/H<sub>2</sub> oxidation using laser absorption of NH<sub>3</sub> and H<sub>2</sub>O, Proc. Comb. Instit. 39 (2023) 233–241
- [9] A.R. Ravishankara, J.S. Daniel, R.W. Portmann, Nitrous oxide (N<sub>2</sub>O): the dominant ozone-depleting substance emitted in the 21st century, Science Science 326 (2009) 123–125
- [10] E.C. Okafor, K.D.K.A. Somarathne, A. Hayakawa, et al., Towards the development of an efficient low-NOx ammonia combustor for a micro gas turbine, Proc. Combust. Inst. 37 (2019) 4597–4606.
- [11] N. Fujii, S. Uchida, H. Sato, S. Fujimoto, H. Miyama, High-temperature reaction of NH<sub>3</sub>-N<sub>2</sub>O System in shock waves, Bull. Chem. Soc. Jpn. 59 (1986) 3431–3437.
- [12] W. Liao, Z. Chu, Y. Wang, S. Li, B. Yang, An experimental and modeling study on auto-ignition of ammonia in an RCM with N<sub>2</sub>O and H<sub>2</sub> addition, Proc. Combust. Inst. 39 (2023) 4377–4385.
- [13] X. Han, M. Lubrano Lavadera, A.A. Konnov, An experimental and kinetic modeling study on the laminar burning velocity of NH<sub>3</sub>+N<sub>2</sub>O+air flames, Combust. Flame 228 (2021) 13–28.
- [14] R.E. Cornell, M.C. Barbet, M.P. Burke, Toward a more comprehensive understanding of the kinetics of a common biomass-derived impurity: NH<sub>3</sub> oxidation by N<sub>2</sub>O in a jet stirred reactor, Energy Fuels 35 (2021) 13338–13348.
- [15] S. Salimian, R.K. Hanson, C.H. Kruger, Ammonia oxidation in shock-heated NH<sub>3</sub>-N<sub>2</sub>O-Ar mixtures, Combust. Flame 56 (1984) 83–95.
- [16] Z. Weng, R. Mével, N. Chaumeix, Detonation in ammonia-oxygen and ammonianitrous oxide mixtures, Combust. Flame 251 (2023) 112680.

- [17] E.L. Petersen, M.J.A. Rickard, M.W. Crofton, E.D. Abbey, M.J. Traum, D.M. Kalitan, A facility for gas- and condensed-phase measurements behind shock waves, Meas. Sci. Technol. 16 (2005) 1716–1729.
- [18] P. Feng, M. Lee, D. Wang, Y. Suzuki, Ammonia thermal decomposition on quartz and stainless steel walls, Int. J. Hydrogen Energy 48 (2023) 29209–29219.
- [19] S.A. Alturaifi, E.L. Petersen, Ammonia line strengths and  $N_{2^+}$ ,  $O_{2^-}$ ,  $Ar_+$ , He-, and self-broadening coefficients in the  $\nu_2$  band near 10.4  $\mu$ m, J. Quant. Spec. Rad. Trans. 262 (2021) 107516.
- [20] X. Zhang, S.P. Moosakutty, R.P. Rajan, M. Younes, S.M. Sarathy, Combustion chemistry of ammonia/hydrogen mixtures: jet-stirred reactor measurements and comprehensive kinetic modeling, Combust. Flame 234 (2021) 111653.
- [21] O. Mathieu, E.L. Petersen, Experimental and modeling study on the hightemperature oxidation of ammonia and related NOx chemistry, Combust. Flame 162 (2015) 554–570.
- [22] H. Nakamura, S. Hasegawa, T. Tezuka, Kinetic modeling of ammonia/air weak flames in a micro flow reactor with a controlled temperature profile, Combust. Flame 185 (2017) 16–27.
- [23] Y. Zhang, O. Mathieu, E.L. Petersen, G. Bourque, H.J. Curran, Assessing the predictions of a NOx kinetic mechanism on recent hydrogen and syngas experimental data, Combust. Flame 182 (2017) 122–141.
- [24] J. Otomo, M. Koshi, T. Mitsumori, H. Iwasaki, K. Yamada, Chemical kinetic modeling of ammonia oxidation with improved reaction mechanism for ammonia/ air and ammonia/hydrogen/air combustion, Int. J. Hydro. Ener. 43 (2018) 3004–3014.
- [25] Z. Wang, X. Han, Y. He, et al., Experimental and kinetic study on the laminar burning velocities of NH<sub>3</sub> mixing with CH<sub>3</sub>OH and C<sub>2</sub>H<sub>5</sub>OH in premixed flames, Combust. Flame 229 (2021) 111392.
- [26] G.J. Gotama, A. Hayakawa, E.C. Okafor, et al., Measurement of the laminar burning velocity and kinetics study of the importance of the hydrogen recovery mechanism of ammonia/hydrogen/air premixed flames, Combust. Flame 236 (2022) 111753.
- [27] D.E. Thomas, K.P. Shrestha, F. Mauss, W.F. Northrop, Extinction and NO formation of ammonia-hydrogen and air non-premixed counterflow flames, Proc. Combust. Inst. 39 (2023) 1803–1812.
- [28] J. Jian, H. Hashemi, H. Wu, P. Glarborg, Study of ammonia oxidation with ozone addition, Appl. En. Combust. Sci. 14 (2023) 100137.
- [29] A. Stagni, S. Arunthanayothin, M. Dehue, et al., Low- and intermediate-temperature ammonia/hydrogen oxidation in a flow reactor: Experiments and a wide-range kinetic modeling, Chem. Eng. J. 471 (2023) 144577.
- [30] M. Baigmohammadi, V. Patel, S. Nagaraja, et al., Comprehensive experimental and simulation study of the ignition delay time characteristics of binary blended methane, ethane, and ethylene over a wide range of temperature, pressure, equivalence ratio, and dilution, Energy Fuels 34 (2020) 8808–8823.
- [31] C.R. Mulvihill, S.A. Alturaifi, E.L. Petersen, A shock-tube study of the N<sub>2</sub>O + M

  N<sub>2</sub> + O + M (M= Ar) rate constant using N<sub>2</sub>O laser absorption near 4.6 μm,

  Combust. Flame 224 (2021) 6–13.
- [32] T. Harada, Y. Murakami, K. Tamaoki, et al., N<sub>2</sub>O consumption by thermal decomposition and reduction with CH<sub>4</sub>, C<sub>2</sub>H<sub>6</sub> and NH<sub>3</sub>, Combust. Sci. Technol. (2023), https://doi.org/10.1080/00102202.2023.2289061.
- [33] A.W. Jasper, Predicting third-body collision efficiencies for water and other polyatomic baths, Farad. Discuss. 238 (2022) 68–86.